國立臺灣海洋大學食品科學系碩士班

專題討論書面報告

TGF-β Signaling in Cartilage Proliferation and Osteoarthritis

授課老師：柯源悌 老師

張君如 老師

指導老師：龔瑞林 老師

學 生：王培瑜 (5123)

老師簽章：

內容 40%	時間掌控 10%	表達能力 30%	投影片 10%	書面資料 10%

報告日期：110 年 3 月 10

TGF-β Signaling in Cartilage Proliferation and Osteoarthritis

王培瑜（**5123**）

2021/3/10

大綱

1. Transforming growth factor-beta1 promotes articular cartilage repair through canonical Smad and Hippo pathways in bone mesenchymal stem cells.
2. TGF-β dampens IL-6 signaling in articular chondrocytes by decreasing IL-6 receptor expression.
3. Controlling joint instability after anterior cruciate ligament transection inhibits transforming growth factor-beta-mediated osteophyte formation.
4. Conclusion

摘要

轉化生長因子（Transforming growth factor beta, TGF-β1）是一種軟骨形成因子，TGF-β1 通過 Smad 路徑 (Mothers against decapentaplegic pathway) 有助於軟骨細胞骨髓間質幹細胞（Bone marrow stem cell, BMSCs）分化，促進軟骨缺陷之早期修復。此外，TGF-β1 抑制軟骨細胞肥大通過 Hippo 信號減少肥大基因的表現。使用 TGF-β1 可以使軟骨修復和再生。白介素-6（Interleukin, IL-6）為促炎細胞因子，與軟骨變性有關，TGF-β 降低 IL-6R 的表達，從而抑制軟骨細胞中 IL-6 誘導 p-STAT3 和下游的 SOCS3 (Suppressor of cytokine signaling 3)、BCL3 (BCL3 Transcription Coactivator)、SAA1 (Serum Amyloid A1) 及 MMP1 (Matrix metalloproteinase-1) 的表現，這顯示了 TGF-β 可能限制促炎性 IL-6 作用以對保持軟骨穩定起重要作用。機械應力是骨關節炎 (Osteoarthritis, OA) 進程中最重要的因素之一。關節的不穩定會導致軟骨損傷和骨贅 (Osteophyte) 形成，可在滑膜 (Synovial membrane) 中觀察到細胞增生和滑膜增厚。因此控制關節不穩定會降低 TGF-β1 和 Smad2/3 的表達，會抑制滑膜細胞的增生，抑制了膝蓋骨中的骨贅的形成和軟骨的變性。綜合上述，TGF-β1 可以促進軟骨的修復，抑制軟骨細胞肥大機制，阻斷 IL-6 下游相關因子的表現，降低軟骨損傷和骨贅的形成。

一、 前言

骨關節炎 (Osteoarthritis, OA) 是常見的退化性疾病，會造成關節疼痛，活動力下降，是成人殘疾最常見的原因之一。TGF-β1 (Transforming growth factor-beta1) 是軟骨形成的誘發因子，可以促進軟骨細胞的增殖和成熟並改善第二型膠原蛋白和蛋白聚醣的堆積。另外，TGF-β1 是具多效型作用，主要對炎症、血管生成、纖維化和腫瘤進展多重作用，並對免疫部位起主要的免疫抑制作用 (Chen *et al*., 2019)。軟骨組織再生中主要經過 Hippo 信號傳導路徑，而 Hippo 信號傳導路徑是由 MST1/2 (Mammalian sterile 20-like kinase 1) 和 LATS1/2 (Large tumor suppressor kinase 1/2) 及轉錄共激活因子 YAP (Yes-associated protein 1) 和 TAZ (Transcriptional coactivator with PDZ binding domain) 組成，而上述因子主要調控細胞增殖、存活、遷移、分化轉錄途徑 (Ma *et al*., 2019)。本次專討的目的，探討 TGF-β1 信號傳導在骨關節炎造成的機制影響。

二、Transforming growth factor-beta1 promotes articular cartilage repair through canonical Smad and Hippo pathways in bone mesenchymal stem cells. (Ying *et al*., 2018)

此篇研究 TGF-β1 長期促進軟骨缺損修復和抑制軟骨細胞肥大分子機制。OA 通常會讓軟骨缺損，目前與藥物有關的治療僅限於改善疼痛和炎症，因此 MSC (Mesenchymal stem cells) 有望重生軟骨缺陷。本篇研究為體外實驗，首先進行實驗，骨髓間充質幹細胞 (Bone marrow stem cell, BMSCs) 是從無菌環境中的 SD (Sprague-Dawley) 雄性四週齡大鼠之雙側脛骨 (Tibia) 提取，再用無菌水 PBS (Phosphate buffered saline) 沖洗，再用 10 mL 血清沖洗，培養在 DMEM (Dulbecco's modified eagle medium)，使用 200 mesh 膜過濾分離細胞，1000 rpm 離心五分鐘，使用 10%的胎牛血清 (Fetal bovine serum, FBS)、1%青黴素/鏈黴素，並在溫度 37°C 和 5% CO_2 下培養，將 BMSCs 從細胞混合物中分離出來，使用 Trypsin -EDTA (Disodium ethylenediaminetetraacetic acid) 消化細胞，達到 90% confluence，培養純化到三代。使用 Lentivirus-EGFP (Enhanced green fluorescent protein) 和 Lentivirus-TGF-β1-EGFP 轉染 (Transfected)，分別轉染到第三代的 BMSCs 中，經培養 72 小時後使用顯微鏡觀察。在上述培養液中培養，並分為三組進行實驗：對照組（無轉染）、載體組（經 Lentivirus-EGFP）和 TGF-β1 組別 (經 Lentivirus-TGF-β1-EGFP)。進行體外實驗，選用 SD 12 週齡雄性大鼠，進行 OA 手術後，分為三組 (一組 12 隻分別為手術後 4 週和 8 週)：模型組 (Model group)、BMSCs group、BMSCs + TGF-β1 group。手術處理後分別治療 4 週和 8 週分批進行犧牲，採集進行組織學 (Histology)、免疫組織化學染色 (Immunohistochemistry)、基因定量分析、Western blot analysis、統計分析。

經由 Fig. 1A 可以觀察到 BMSCs/calcium alginate gel alone 的形成的情形；Fig. 1B 為顯微鏡下觀察 BMSCs/calcium alginate gel alone. Fig. 2A 黑色箭頭顯示在第 4 週和第 8 週軟骨修復圖示，由肉眼觀察手術後第 4 週和第 8 週軟骨損傷尚未完全修復，在 BMSCs group 表面較粗糙，但周圍乾淨；而 BMSCs + TGF-β1 group 表面完整，具有良好修復性。經由 Fig. 2B 在 ICRS (International cartilage repair scores) 評分中 BMSCs + TGF-β1 group 分數高於 Model group 和 BMSCs group，證明 BMSCs + TGF-β1 group 具良好修復性。經由 Fig. 3 TGF-β1 轉染 BMSCs 有效促進軟骨修復情況，Fig. 3A 為了觀察細胞結構和基質在不同組別的差別，使用 ABH Antibody 和 IHC (Immunohistochemistry) 對糖胺聚醣、第二型膠原蛋白進行染色，在 BMSCs + TGF-β1 group 中糖胺聚糖 (Glycosaminoglycan, GAGs) 覆蓋較多。Fig. 3B 在 Mankin 評分表示第 4 週和第 8 週 model group 比 BMSCs + TGF-β1 group 還高，但 model group 和 BMSCs group 沒有顯著差異，顯示 BMSCs + TGF-β1 group 與正常軟骨組織較相似。經由 Fig. 3C IHC 染色結果得知第二型膠原蛋白在 model group 中較不明顯，但在 BMSCs + TGF-β1 group 覆蓋高於 BMSCs group；Fig. 3D 為使用 PCR (Polymerase chain reaction) 螢光定量檢測修復軟骨組織中的 Col2a1 為第二型膠原蛋白 alpha1 鏈，結果表明 BMSCs + TGF-β1 group Col2a1 高於其他組別。經由 Fig. 4 分析可以確認是否經由 Lentivirus-TGF-β1-EGFP 轉染激活 TGF-β1 依賴性的 Smad2/3 信號傳導，讓 BMSCs 中細胞內信號傳導誘導軟骨分化。Fig. 4A 紅色箭頭為 p-smad2 (Phospho-Smad2) 陽性細胞，在第 4 週 p-smad2 表現不明顯，其中 BMSCs group 微弱增強，在 Lentivirus-TGF-β1-EGFP 明顯增強。Fig. 4B 使用螢光顯微鏡測得 Lentivirus-TGF-β1-EGFP 轉染處理在第 4 週強烈激活 p-smad2。Fig. 4C 經由 Lentivirus-TGF-β1-EGFP 可增強 p-smad2，顯示 TGF-β1 誘導增加軟骨形成分子的表現，與 Fig. 3D 之結果相符。經由體外實驗，Western blot analysis 結果得知 Lentivirus-TGF-β1-EGFP 轉染增加 p-smad2/3 的信號傳導。經由 Fig. 5 確認 TGF-β1 通過調節 Hippo 信號傳導路徑是否抑制軟骨肥大。Fig. 5A、5B 分析結果得知 Lentivirus-TGF-β1-EGFP 轉染結果 YAP-1 (Yes-associated protein 1) 顯著增加，在抑制肥大軟骨淋巴細胞 Runx2、Col10 的表現。

結果此篇研究證明經由 Lentivirus-TGF-β1-EGFP 轉染的 BMSCs/calcium alginate gel 依賴 Smad2/3 信號傳導及 Hippo 信號傳導可促進軟骨缺損及再生、抑制肥大細胞。

三、 TGF-β dampens IL-6 signaling in articular chondrocytes by decreasing IL-6 receptor expression. (Wiegertjes *et al.*, 2019)

TGF-β1 是重要的軟骨穩定調節劑，相反的 IL-6 (Interleukin 6) 是一種促炎細胞因子，與軟骨變性有關。此篇研究軟骨細胞中 TGF-β1 對 IL-6 信號傳導調節作用。IL-6 分為經典路徑 (Classic signaling) 和反經典路徑 (Trans signaling)，IL-6R (IL-6 receptor) 使 IL-6 的功能多樣性。從七名 OA 患者，分離出原代人軟骨細胞，培養在 DMEM/F12 (Dulbecco's modified eagle medium/nutrient mixture F-12) medium 中以 1.5mg/ml Collagenase B 消化過夜，軟骨細胞以 1×10^5 cells/cm^2 的密度接種在 6-well plates 中進行蛋白質試驗，或在 24-well plates 中進行基因試驗。在添加 10%的胎牛血清、100 mg/L 丙酮酸、100 U/ml 青黴素和 100 mg/mL 鏈黴素的 DMEM/F12 培養在 5% CO2 (v/v)，37ºC，95% 濕度一週。G6 chondrocytes 自 OA 供體的脛骨軟骨，通過溫度依賴的 SV40 癌基因進行轉導，因此 G6 軟骨細胞於 32 ºC 下培養，使用 5% FCS。以 rhTGF-β1(Recombinant Human Transforming Growth Factor beta 1)、rhIL-1β (Recombinant Human Interleukin-1 beta)、rhIL-6 (Recombinant Human Interleukin-6)及 rhIL-6R (Recombinant Human Interleukin-6 receptor) 使用這些組合刺激原代軟骨細胞和 G6 軟骨細胞。抑制劑實驗中使用 0.05% (v/v) DMSO (Dimethyl sulfoxide) 作為對照組，抑制 ALK5 kinase (Activin receptor-like kinase 5)、JAK (Janus kinase) 及 IL-6R 活性，使用 SB-505124、Tofacitinib、Tocilizumab 抑制劑。使用 Luminex 技術進行蛋白質測量、Western blot、PCR (Polymerase chain reaction)、統計分析。

Fig. 6 TGF-β1 刺激在人 G6 軟骨細胞中迅速誘導 IL-6，使用 qPCR 進行基因表達。Fig. 6A 顯示 IL-6 顯著增加；Fig. 6B 為了驗證 Fig. 6A 結果，在 4 個不同供體分離原代軟骨細胞，觀察之間變化，TGF-β1 顯著增加，IL-6 平均 4 小時增加 32 倍、6 小時增加 74 倍。Fig. 6C 在蛋白質含量上進一步證實上述結果，TGF-β1 刺激 G6 軟骨細胞 IL-6 顯著增加 20 倍。Fig. 7 TGF-β1 刺激導致 STAT3 (Signal transducer and activator of transcription 3) 磷酸化，這取決於 IL-6R 以及 ALK5 和 JAK kinase 活性。Fig. 7A 為了研究 TGF-β1 誘導的 IL-6 是否導致自分泌信號傳導，研究了 IL-6R 下游信號傳導蛋白 p-STAT3 的模式，在 TGF-β1 刺激 G6 軟骨細胞的 2 小時和 4 小時 p-STAT3 明顯增加。Fig. 7B 為了測試 TGF-β1 誘導的 p-STAT3 使否為 IL-6R 依賴性，使用 IL-6R 的抑制劑 Tocilizumab 進行測驗，TGF-β 對 p-STAT3 的誘導被抑制。Fig. 7C 進一步分析參與 TGF-β1 誘導 IL-6 和 p-STAT3 信號蛋白，以 ALK5 kinase 之抑制劑 SB-505124，在所有時間點上抑制 p-Smad2/3 和 p-STAT3。Fig. 7D 使用 JAK 抑制劑 Tofacitinib 可以完全抑制 TGF-β1 誘導 p-STAT3。這表明 TGF-β1 誘導 p-STAT3 取決於 IL-6R 以及 ALK5-和 JAK 激酶活性。Fig. 8 TGF-β1 阻斷 IL-6 介導的 SOCS3 基因表達並限制 STAT3 磷酸化。為了觀察 STAT3 磷酸化是否導致基因轉錄，測量 STAT3 目標基因

SOCS3 的 mRNA，SOCS3 本身是 IL-6 重要調控因子。Fig. 8A 為了研究 TGF-β1 誘導 IL-6 的下游效應，將 G6 軟骨細胞在抑制劑 Tocilizumab 抑制 IL-6 信號傳導，並 TGF-β1 刺激，測量 SOCS3 的表達，TGF-β1 沒有增加 SOCS3 基因表現，但單獨使用重組 IL-6 刺激增加三倍 SOCS3 基因表現。這表明 TGF-β1 阻斷了 IL-6 誘導的 SOCS3 基因表現。Fig. 8B 為了證實 TGF-β1 確實抑制重組 IL-6 作用，將 TGF-β1 進行六小時預處理，模擬細胞暴露先在 TGF-β1，然後再暴露 IL-6，STAT3 在預處理 TGF-β1 被抑制。Fig. 8C TGF-β1 預處理完全抑制 SOCS3。這表明 TGF-β1 阻斷 IL-6 介導 SOCS3 基因表現並限制 p-STAT3。Fig. 9 TGF-β1 有效降低 G6 軟骨細胞和原代軟骨細胞中 IL-6R 的水平。Fig. 9A 觀察到 TGF-β1 刺激導致 IL-6R 在四小時和六小時下降，Fig. 9B TGF-β1 對 IL-6R 在不同供者的原代軟骨細胞也是如此。Fig. 9C 研究刺激 IL-6 產生的其他因素使否也可以調節 IL-6R，使用 IL-6 的誘導劑 IL-1β (Interleukin-1 beta)，IL-1β 顯著提高 IL-6，與 TGF-β1 相反 IL-1β 並未顯著改變 IL-6R 的表現。表示 IL-6 不會參與 IL-6R 的調控。Fig. 9D TGF-β1 刺激 G6 軟骨細胞 24 小時後 IL-6R 降低，而 IL-1β 升少量鄰佳 IL-6R。這些數據表明 TGF-β1 降低 IL-6R。Fig. 10 TGF-β1 通過降低 IL-6R 的水平來阻斷 IL-6 的反應。Fig. 10A TGF-β1 經過 6 小時的預處理，添加可溶性的 IL-6R，p-STAT3 跟著 IL-6R 劑量而增加。Fig. 10B TGF-β1 和 IL-6R 恢復了 IL-6 對 SOCS3 的誘導。其他 IL-6 反應基因 MMP1，BCL3 和 SAA1 的表達也受到相同的調節。

結果 TGF-β1 誘導人關節軟骨細胞中 IL-6 的釋放。釋放的 IL-6 以自分泌方式與軟骨細胞上的膜結合 IL-6 受體結合，並導致細胞內信號傳導介質 STAT3 磷酸化。同時，TGF-β1 降低了軟骨細胞上 IL-6R 的表達，導致 STAT3 磷酸化受到限制，並抑制 STAT3 反應性靶基因 (Fig. 11)。

四、Controlling joint instability after anterior cruciate ligament transection inhibits transforming growth factor-beta-mediated osteophyte formation. (Murata *et al*., 2019)

此篇研究 OA 誘導不穩定模型與穩定模型，評估大鼠滑膜中骨贅的形成是否經由 TGF-β 的 Smad2/3 路徑和 BMP-2 (Bone morphogenetic protein-2) 的 Smad 1/5/8 路徑。Fig. 12 實驗設計將 96 隻 12 週齡 Wistar 雄性大鼠，分為兩組：CAM group、SHAM group，進行 ACL (Anterior cruciate ligament) 手術 Fig. 12B，穩定組為 CAM group 透過尼龍繩緊綁模擬關節穩定，不穩定組為 SHAM group 透過尼龍繩鬆綁模擬關節不穩定，分別在 2、4、8 週進行 X-ray、組織學分析、免疫

組織化學分析、免疫螢光分析、ELISA (Enzyme-linked immunosorbent assays)、統計分析。

Fig. 13 手術後關節不穩定評估。Fig. 13A 在手術後 2、4、8 週關節不穩定放射線圖，SHAM group 脛骨明顯向前位移。Fig. 13B CAM group 在 2、4 週明顯抑制脛骨前端不穩定，第 8 週 SHAM 和 CAM group 沒有差異。Fig. 14 控制關節不穩定情形，延緩軟骨惡化。Fig. 14A 使用蘇木精及番紅染色軟骨組織切片，白色箭頭指軟骨 Pannus，黑色箭頭為 Cluster cells，觀察到 SHAM group 在 4、8 週軟骨的惡化、表面纖維化；Fig. 14B 使用 Mankins 評分 SHAM group 在 4、8 週高於 CAM group，表示控制穩定關節抑制軟骨惡化，表面纖維化。Fig. 14C SHAM group 染色切片中顯示 TGF-β1 高於 CAM group，但是在第八週 SHAM group 面積並不比 CAM group 高；相比之下，兩組之間的 BMP-2 相差不明顯。Fig. 15 關節不穩定受到控制，顯示出滑膜炎和滑膜增厚受到抑制，在 Fig. 15A 使用蘇木精和番紅染色，與 SHAM group 相比，CAM group 在 4 週和 8 週細胞層數量變少，並抑制滑膜組織的增殖；但是 Fig. 15B 在兩組的炎症評分沒有顯著差異，兩組在 TGF-β1、BMP-2 表達均不明顯。Fig. 16 ELISA 檢測 TGF-β1、BMP-2 的蛋白表現，Fig. 16A 術後 8 週組間差異無統計學意義，對於 BMP-2 表現，各組在任何時間點均無顯著的差異。Fig. 17 控制關節穩定抑制骨贅的形成。Fig. 17A SHAM group 半定量評分顯著高於 CAM group，Fig. 17B 使用番紅固綠染色 (Safranin O/fast green stains) 對脛骨組織染色，黑色箭頭為脛骨的軟骨和骨贅的形成。經由骨贅評分，CAM group 骨贅的大小、總分受到抑制。Fig. 18 受到控制關節抑制軟骨化生 (cartilage metaplasia) 中的 p-Smad2/3 和 p-Smad 1/5/8 表現。Fig. 18A 與 CAM group 相比，SHAM group 的表現量更大；Fig. 18B 螢光密度評分，在手術後第 4 週、第 8 週 CAM group 軟骨組織的化生、p-Smad2/3 及 p-Smad 1/5/8 的表現受到抑制。

結果，不穩定的關節會使軟骨表面纖維化、肥大細胞和炎症細胞增加，穩定的關節會增加 TGF-β1 抑制骨贅生成。

五、結論

1. 經由 Lentivirus-TGF-β1-EGFP 轉染增加 YAP-1，抑制肥大軟骨淋巴細胞 Runx2、Col10 的表達。
2. TGF-β1 誘導人關節軟骨細胞中 IL-6 的釋放，並抑制 p-STAT3。
3. 控制關節穩定，會增加 TGF-β1 抑制骨贅生成和肥大細胞。

六、參考資料

Ying, J., Wang, P., Zhang, S., Xu, T., Zhang, L., Dong, R., Xu, S., Tong, P., Wu, C., & Jin, H. (2018). Transforming growth factor-beta1 promotes articular cartilage repair through canonical Smad and Hippo pathways in bone mesenchymal stem cells. *Life Sciences*, *192*, 84-90.

Wiegertjes, R., Van Caam, A., Van Beuningen, H., Koenders, M., Van Lent, P., Van Der Kraan, P., van de Loo, F., & Davidson, E. B. (2019). TGF-β dampens IL-6 signaling in articular chondrocytes by decreasing IL-6 receptor expression. *Osteoarthritis and Cartilage*, *27*(8), 1197-1207.

Murata, K., Kokubun, T., Onitsuka, K., Oka, Y., Kano, T., Morishita, Y., Ozone, K., Kuwabara, N., Nishimoto, J., & Isho, T. (2019). Controlling joint instability after anterior cruciate ligament transection inhibits transforming growth factor-beta-mediated osteophyte formation. *Osteoarthritis and Cartilage*, *27*(8), 1185-1196.

Chen, S., Liu, S., Ma, K., Zhao, L., Lin, H., & Shao, Z. (2019). TGF-β signaling in intervertebral disc health and disease. *Osteoarthritis and Cartilage*, *27*(8), 1109-1117.

Chen, Y., Di, C., Zhang, X., Wang, J., Wang, F., Yan, J. f., Xu, C., Zhang, J., Zhang, Q., & Li, H. (2020). Transforming growth factor β signaling pathway: a promising therapeutic target for cancer. *Journal of Cellular Physiology*, *235*(3), 1903-1914.

Kim, H. S., & Lee, M.-S. (2007). STAT1 as a key modulator of cell death. *Cellular Signalling*, *19*(3), 454-465.

Ma, S., Meng, Z., Chen, R., & Guan, K.-L. (2019). The Hippo pathway: biology and pathophysiology. *Annual Review of Biochemistry*, *88*, 577-604.

Van der Kraan, P., & Van den Berg, W. (2012). Chondrocyte hypertrophy and osteoarthritis: role in initiation and progression of cartilage degeneration. *Osteoarthritis and Cartilage*, *20*(3), 223-232.

Zhao, B., Li, L., Lei, Q., & Guan, K.-L. (2010). The Hippo–YAP pathway in organ size control and tumorigenesis: an updated version. *Genes & Development*, *24*(9), 862-874.

Budi, E. H., Duan, D., & Derynck, R. (2017). Transforming growth factor-β receptors and Smads: regulatory complexity and functional versatility. *Trends in Cell Biology*, *27*(9), 658-672.

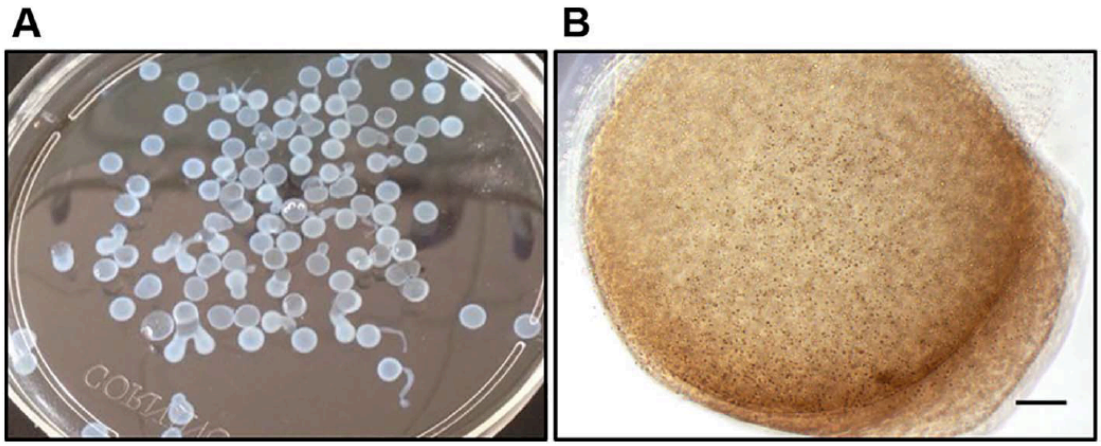

Fig. 1. (A) Gross views of formed BMSCs/calcium alginate gels. (B) Microscopic observation of one formed BMSCs/calcium alginate gel. Bar = 2 mm.

(Ying *et al*., 2018)

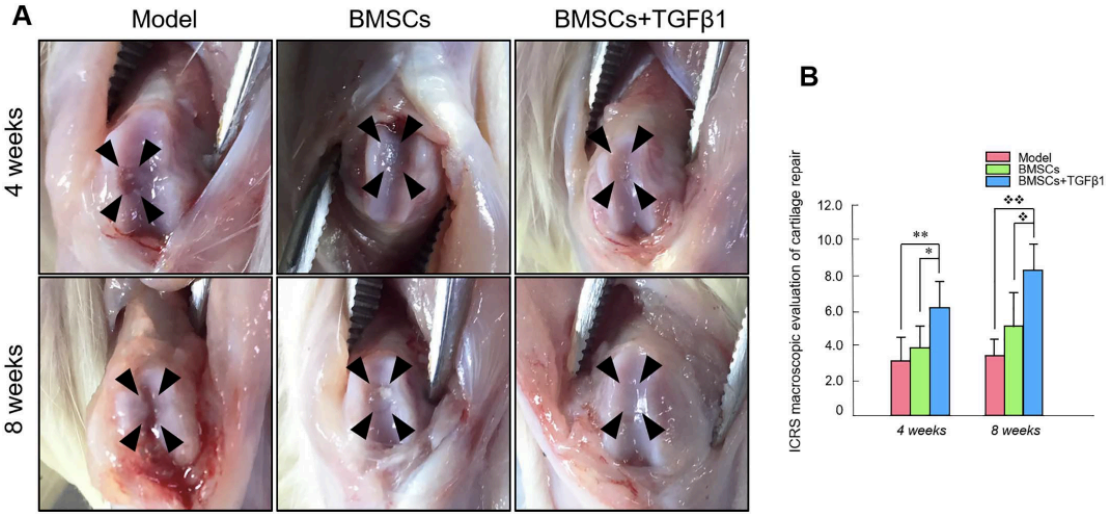

Fig. 2. (A) Representative gross views of repaired cartilage defects at weeks 4 and 8 in the black arrowheads. Defects were left untreated (model group) or treated with non-transfected BMSCs/calcium alginate gel (BMSCs group) and Lentivirus-TGF-β1-EGFP transfected BMSCs/calcium alginate gel (BMSCs +TGF-β1 group). (B) Evaluation of ICRS macroscopic cartilage repair scores. *P < 0.05 and ❖P < 0.05 versus BMSCs + TGF-β1 group, **P < 0.01 and ❖❖P < 0.01 versus BMSCs +TGF-β1 group.

(Ying *et al*., 2018)

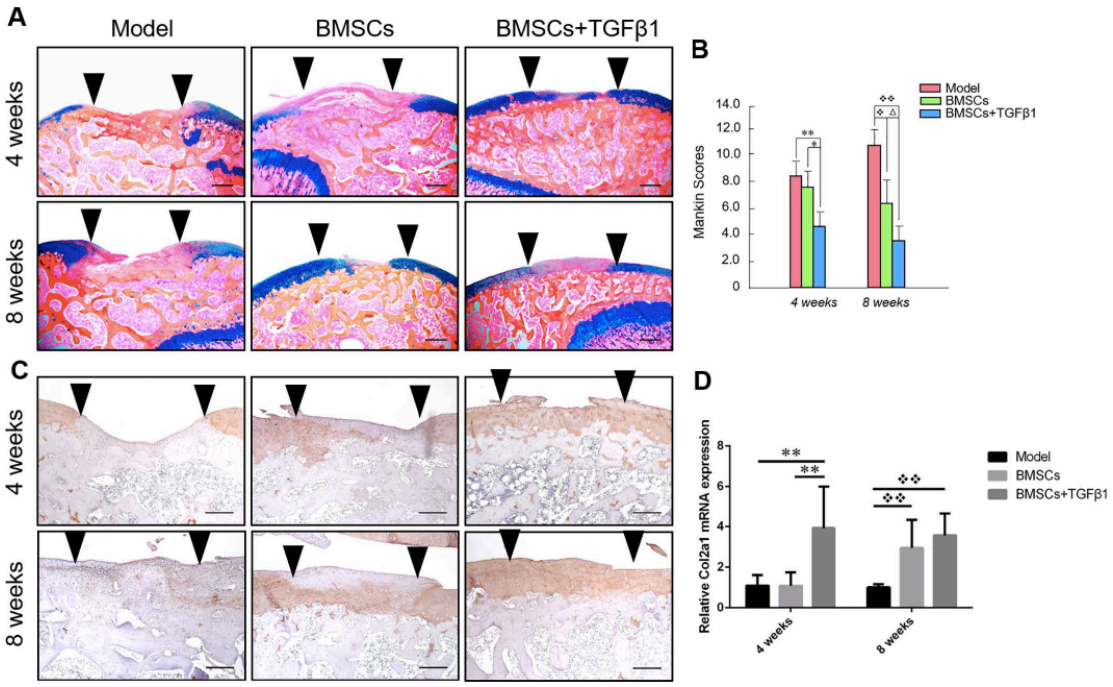

Fig. 3. TGFβ1-transfected BMSCs effectively promote cartilage repairing. (A) Histological sections of repaired cartilage defects stained using Alcian Blue Hematoxylin/Orange G. Black arrowheads indicate repaired regions. Bar =3 mm; (B) Mankin scores of histological repairing cartilages at defect sites; (C) Immunohistochemistry (brown) of collagen type II in repaired regions. Black arrows indicate repaired regions. Bar =1 mm; (D) Total RNA was extracted from repaired tissues at weeks 4 and 8. In BMSCs + TGF-β1 group, expression of Col2a1 was significantly increased at 4 and 8 weeks. Data are presented as means ± SD. *P < 0.05 and ▵P < 0.05 versus BMSCs + TGF-β1 group, ❖P < 0.01 versus BMSCs group, **P < 0.01 versus BMSCs +TGF-β1 group and ❖❖P < 0.01 versus model group. (For interpretation of the references to color in this figure legend, the reader is referred to the web version of this article.)

(Ying *et al*., 2018)

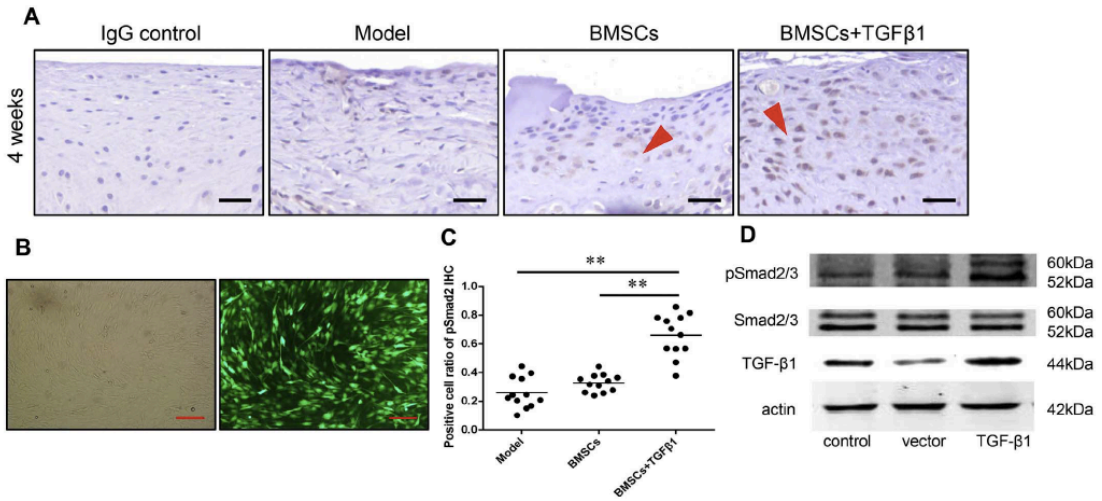

Fig. 4. Overexpression of TGF-β1 promotes the phosphorylation of Smad2/3 in BMSCs during the early repairing progress. (A) IHC of phospho-Smad2 (brown) in repaired regions. Red arrowheads: phospho-Smad2-positive cells. Bar= 50 μm; (B) BMSCs were observed using microscopy with normal and EGFP under the same vision at day 3 following transfection with Lentivirus-TGF-β1-EGFP. Bar=1 mm; EGFP, enhanced green fluorescent protein. (C) Positive cell ratio of phospho-Smad2 was significantly increased in BMSCs +TGF-β1 group (week 4). (D) Western blot analysis demonstrated that Lentivirus-TGF-β1-EGFP was successfully transfected into BMSCs and the protein expression of pSmad2/3 was significantly increased in the BMSCs + TGF-β1 group, compared with the control and vector groups. Data are presented as means ± SD. **P < 0.01 versus BMSCs +TGF-β1 group. (For interpretation of the references to color in this figure legend, the reader is referred to the web version of this article.)

(Ying *et al*., 2018)

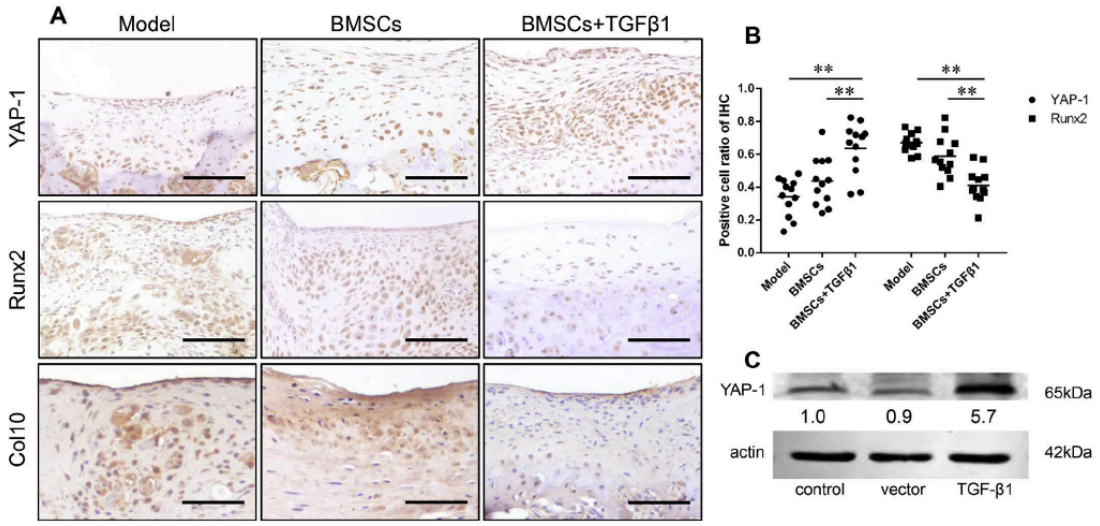

Fig. 5. TGF-β1 decrease hypertrophic markers expression to inhibit chondrocyte hypertrophy by increasing YAP-1 expression at week8. (A) IHC of YAP-1, Runx2 and Col10 (brown) in repaired regions. (B) Positive cell ratio of YAP-1 was significantly increased in BMSCs + TGF-β1 group (week 8). (C) The protein expression of YAP-1 was significantly increased in the BMSCs +TGF-β1 group in vitro, compared with the control and vector groups; Bar= 50 μm; Data are presented as means ± SD. **P < 0.01 versus BMSCs +TGF-β1 group. (For interpretation of the references to color in this figure legend, the reader is referred to the web version of this article.)

(Ying *et al*., 2018)

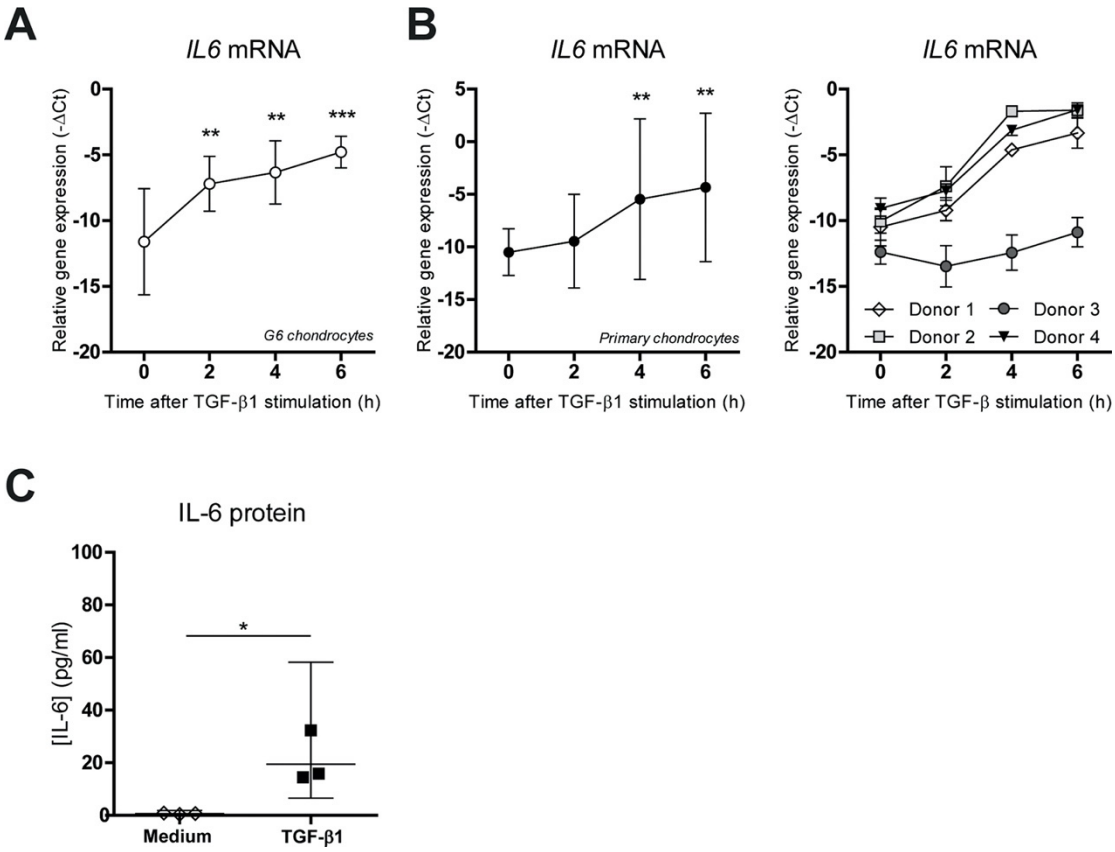

Fig. 6. TGF-β1 stimulation of human chondrocytes rapidly induces IL-6. The human G6 chondrocyte cell line and primary human chondrocytes of four donors were stimulated in triplo with 1.0 ng/ml of rhTGF-β1 for 2, 4 and 6 h to study TGF-β1-induced IL6 gene expression using qPCR. (A) For G6 chondrocytes, the mean of three separate experimental repeats is shown with corresponding 95% confidence interval (CI). (B) For primary chondrocytes, the mean of four donors is shown with corresponding 95% CI, and individual donors are plotted showing mean ± SD of technical replicates (C) G6 chondrocytes were stimulated with 1.0 ng/ml of rhTGF-β1 for 24 h, after which the concentration of IL-6 in the supernatant was measured using Luminex technology. The means of three separate experiments are shown with corresponding 95% CI. * = $P < 0.05$; ** = $P < 0.01$, *** = $P < 0.001$ as measured by repeated measures ANOVA with Dunnett's post-test (A, B) or unpaired two-tailed *t*-test (C).

(Wiegertjes *et al*., 2019)

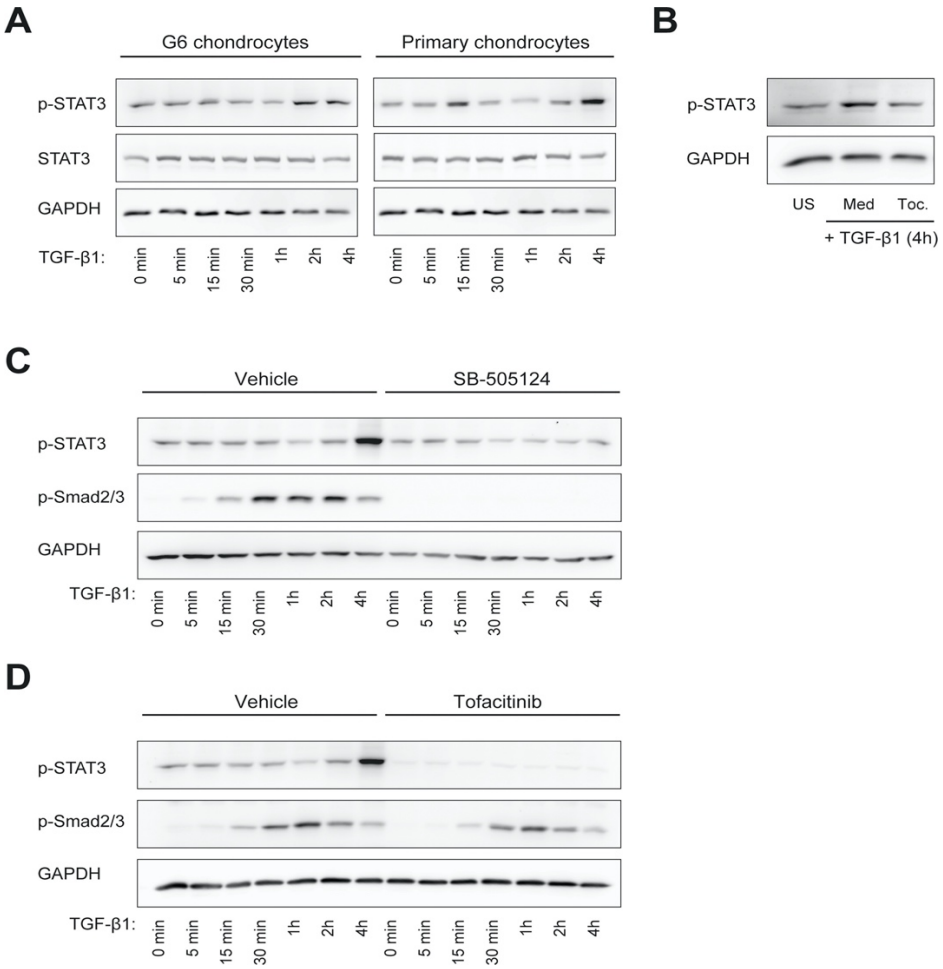

Fig. 7. TGF-β1 stimulation leads to STAT3 phosphorylation, dependent on the IL-6R, as well as ALK5- and JAK-kinase activity. (A) The human G6 chondrocyte cell line and primary human chondrocytes of three donors were stimulated with 1.0 ng/ml of rhTGF-β1 for 5, 15, or 30 min and 1, 2, and 4 h, to study TGF-β1-induced STAT3 phosphorylation with Western Blot. (B) Tocilizumab (anti-IL-6R antibody) was used to investigate if TGF-β1-induced STAT3 phosphorylation was dependent on IL-6R signaling. G6 chondrocytes were pre-incubated with 1 mg/ml of Tocilizumab for 1 h, and afterwards stimulated with 1 ng/ml of rhTGF-β1 for 4 h. Small molecule inhibitors for (C) TGF-β receptor kinase activity (SB-505124, 5 mM) and (D) JAK-kinase activity (Tofacitanib, 1 μM) were used to investigate if TGF-β1-induced STAT3 phosphorylation was dependent on ALK5- or JAK kinase activity respectively. G6 chondrocytes were pre-incubated with inhibitors or vehicle for 1 h, and stimulated with 1 ng/ml of rhTGF-β1 for indicated time points. Western Blots shown are representative of at least three independent experiments. Toc: Tocilizumab; Med: medium; US: unstimulated.

(Wiegertjes *et al*., 2019)

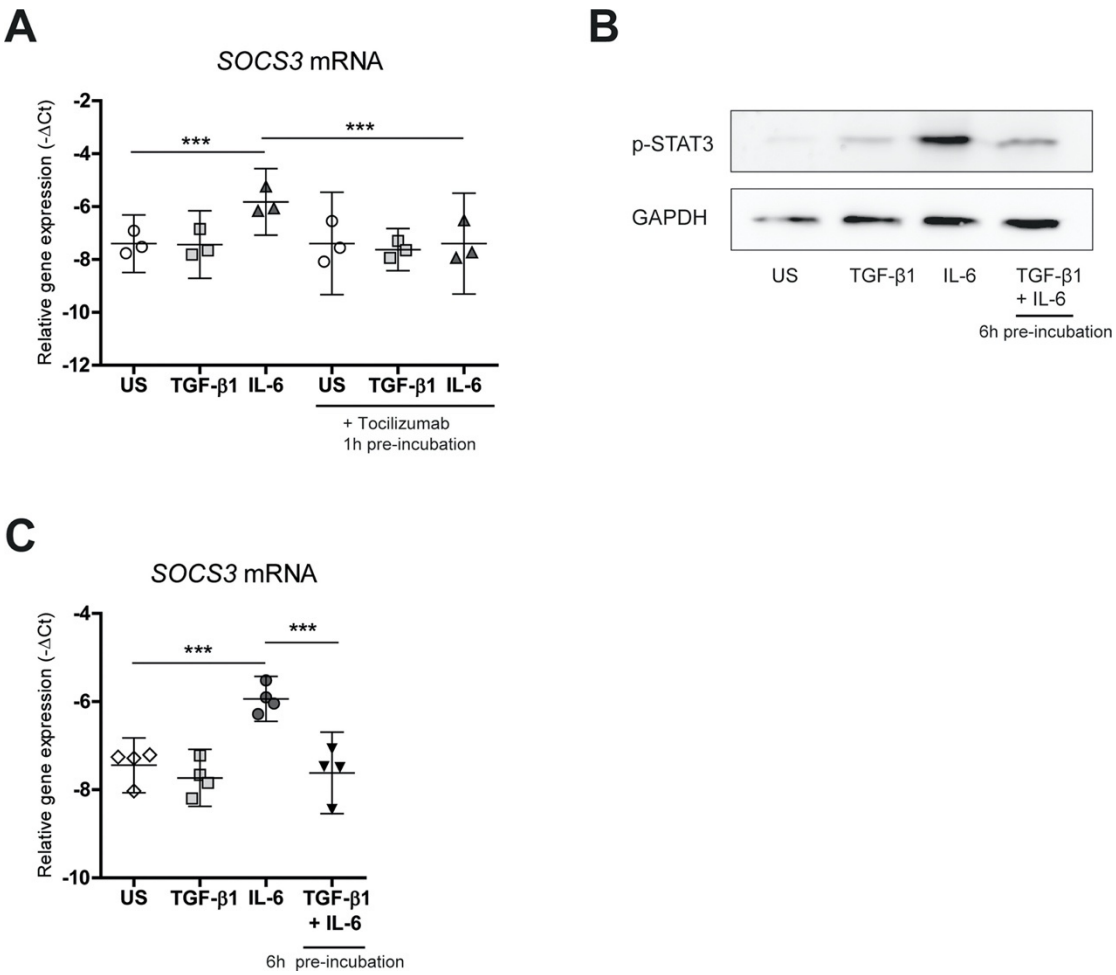

Fig. 8. TGF-β1 blocks IL-6 mediated gene expression of SOCS3 and limits STAT3 phosphorylation. (A) To investigate the downstream effects of TGF-β1-induced IL-6 signaling, G6 chondrocytes were pre-incubated with 1 µg/ml of Tocilizumab to block IL-6R signaling, and stimulated with TGF-β1 for 6 h. Expression level of the STAT3 target gene SOCS3 was measured as a read-out for IL-6-mediated gene expression. (B, C) To study the effect of TGF-β1 on signaling of exogenous rhIL-6, human G6 chondrocytes were pre-stimulated with or without 1.0 ng/ml of rhTGF-β1 for 6 h, and afterwards stimulated with rhIL-6 (10 ng/ml). The IL-6 response was measured by induction of STAT3 phosphorylation after 30 min (B) or induction of SOCS3 mRNA after 6 h (C). Western Blot is representative of three independent experiments. For gene expression results, the means of three or four separate experimental repeates are plotted with corresponding ±95% CI. * =P < 0.05; ** = P < 0.01, *** = P < 0.001 as measured by repeated measurements ANOVA with Bonferroni's posttest.
US: unstimulated.

(Wiegertjes *et al*., 2019)

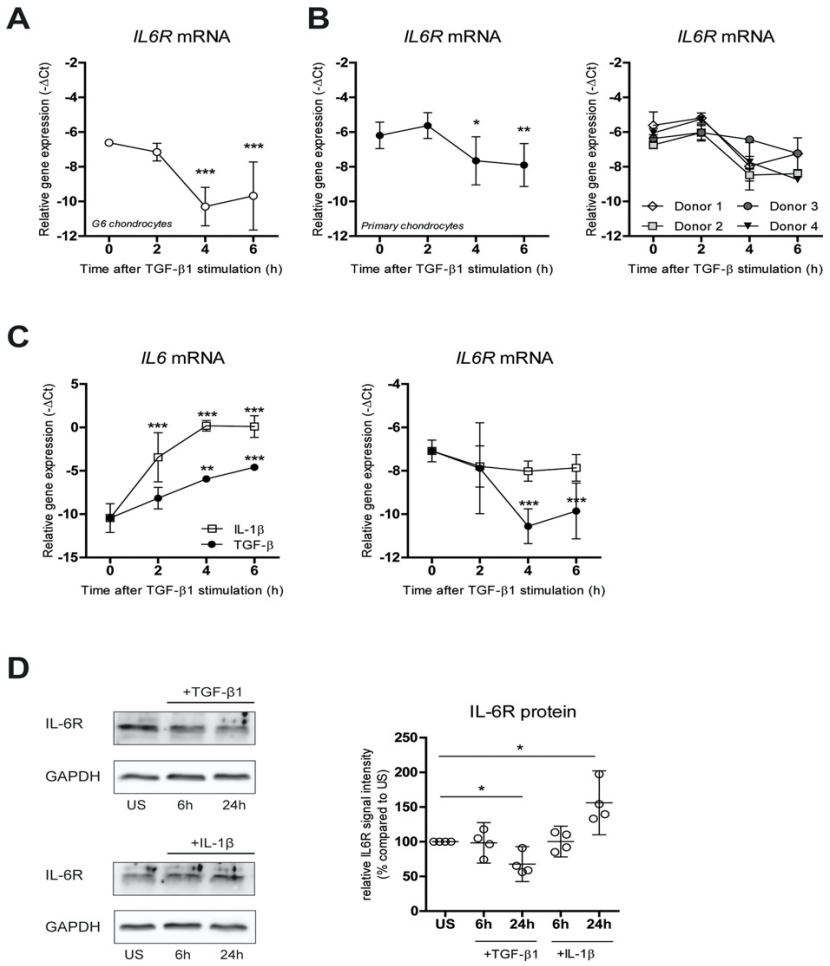

Fig. 9. TGF-β1 potently decreases IL-6 receptor levels in both G6 and primary chondrocytes. To investigate the effect of TGF-β1 on expression of the IL6R, G6 chondrocytes and primary human chondrocytes of four donors were stimulated in triplicate with 1.0 ng/ml of rhTGF-b1 for 2, 4 or 6 h. (A) For G6 chondrocytes, the mean of three separate experimental repeats is shown with corresponding 95% CI. (B) For primary chondrocytes, the mean of four donors is shown with corresponding 95% CI, and individual donors are plotted showing mean ± SD of technical replicates. (C) G6 chondrocytes were stimulated with 1.0 ng/ml of rhTGF-β1 or 1.0 ng/ml of rhIL-1b for 2, 4 or 6 h to study effects on IL6 and IL6R expression. Mean of four separate experimental repeats is shown with corresponding 95% CI. (D) G6 chondrocytes were stimulated with 1.0 ng/ml of rhTGF-β1 or 1.0 ng/ml of rhIL-1b for 6 h and 24 h to determine effects on IL-6R protein expression using Western Blot. Western blots are representative of four independent experiments. Quantification of theWestern Blot was performed by Image J. Quantitative values of IL6R protein intensity were first corrected for GAPDH values, and then plotted as fold change (%) compared to US samples. * = $P < 0.05$; ** = $P < 0.01$, *** = $P < 0.001$ as measured by one-way ANOVA with Dunnett's (A, B, C) or Bonferroni's (D) post-test. US: unstimulated.

(Wiegertjes *et al*., 2019)

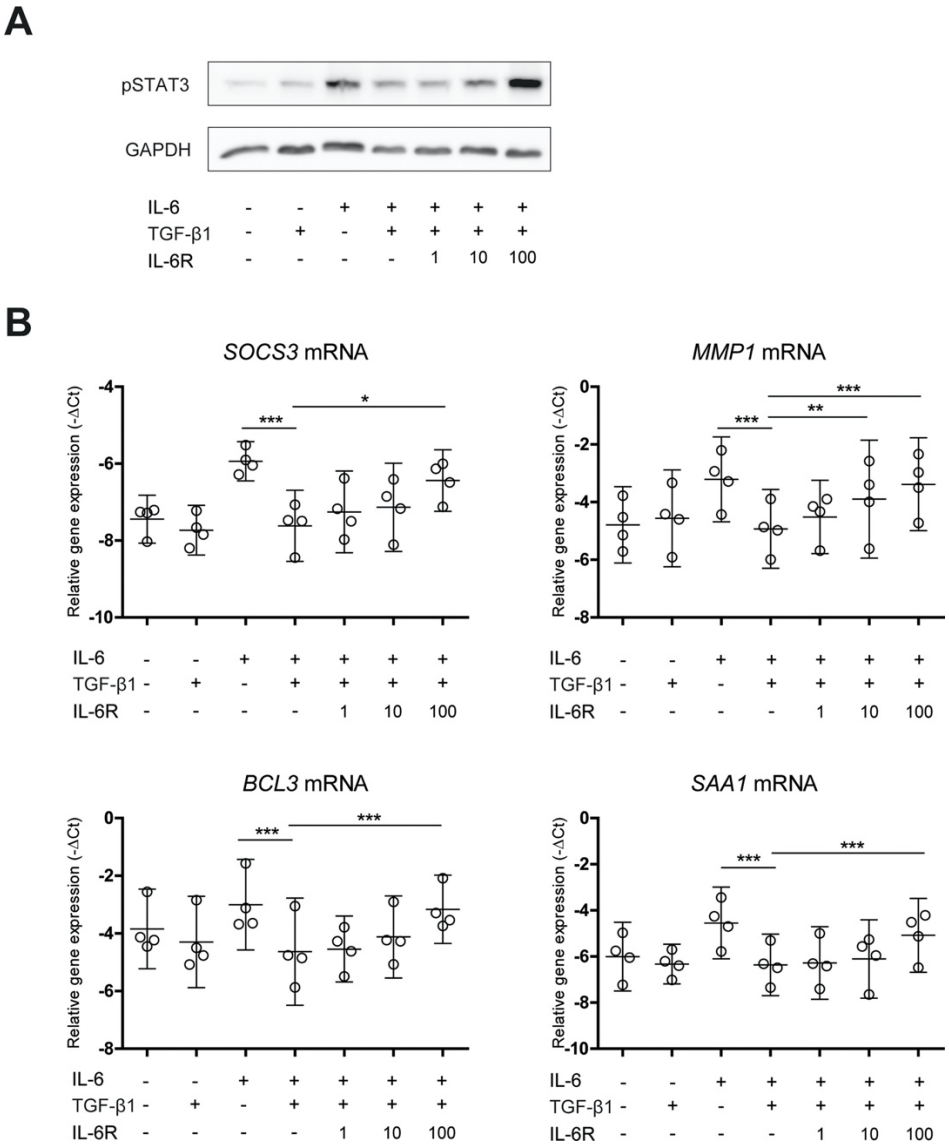

Fig. 10. TGF-β1-mediated inhibition of IL-6 signaling is dependent on decreased IL-6R levels. To study the effect of TGF-β1 on IL-6 signaling with or without recombinant IL-6R, human G6 chondrocytes were pre-stimulated with 10 ng/ml of rhTGF-β1 for 6 h, and afterwards stimulated with rhIL-6 (10 ng/ml) alone or in combination with rhIL-6R (1, 10 and 100 ng/ml). The IL-6 response was measured by induction of p-STAT3 after 30 min of IL-6 stimulation (A) or induction of SOCS3, MMP1, BCL3 and SAA1 expression after 6 h (B). Western blots are representative of three independent experiments. For gene expression studies, the means of four separate experimental repeates are plotted with corresponding ±95% CI. * = P < 0.05; ** = P < 0.01, *** = P < 0.001 as measured by repeated measures ANOVA with Bonferroni's post-test.

(Wiegertjes *et al*., 2019)

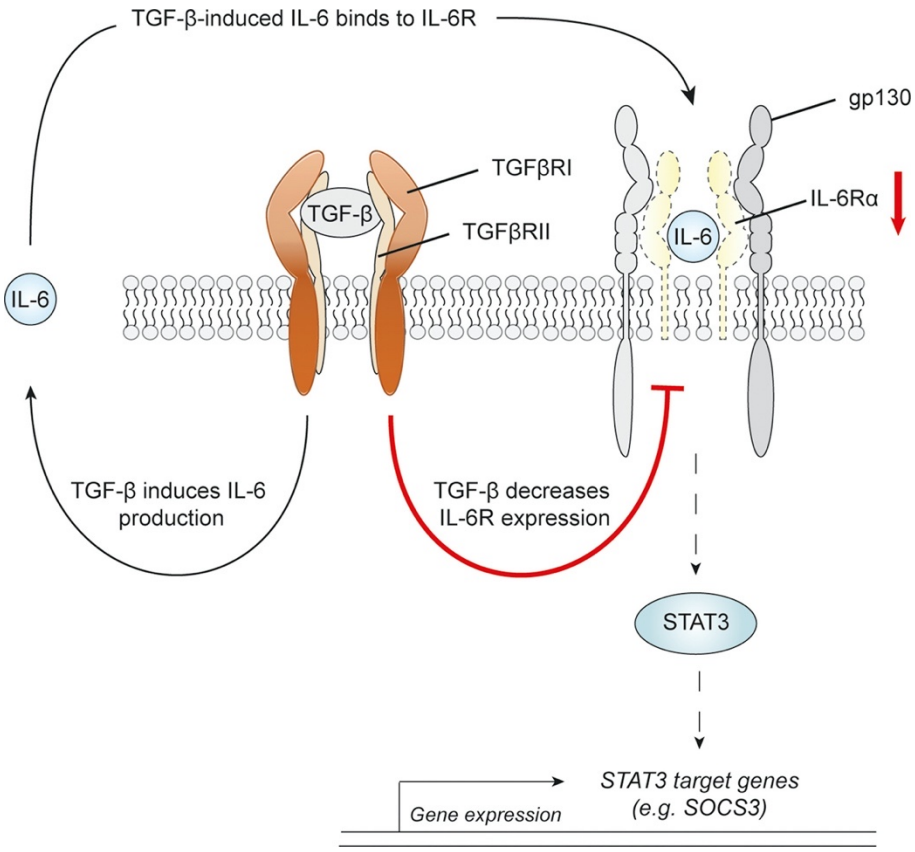

Fig. 11. Schematic overview of TGF-β1-mediated regulation of IL-6 signaling in chondrocytes. TGF-β1 induces the release of IL-6 in human articular chondrocytes. Released IL-6 binds in an autocrine manner to membrane-bound IL-6 receptor on chondrocytes and leads to phosphorylation of the intracellular signaling mediator STAT3. Simultaneously, TGF-β1 decreases IL-6 receptor expression on chondrocytes, resulting in limited STAT3 phosphorylation and inhibition of STAT3-responsive target genes.

(Wiegertjes *et al.*, 2019)

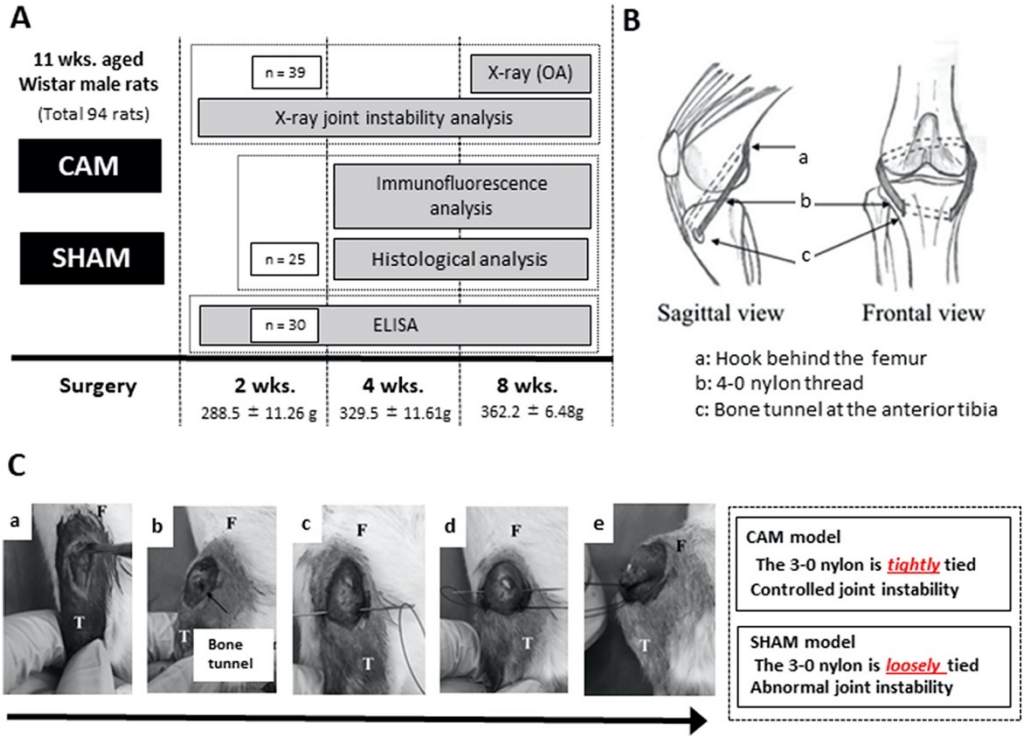

Fig. 12. (A) Study design and timing of the analyses. (B) Schematic representation of the surgical procedure. (C) Surgical protocols for the controlled abnormal joint instability model (CAM group) and continued joint instability model (SHAM group). The models use the same protocol for procedures (a)-(d), but differ in the final procedure (e). Under anesthesia, the right knee joint is exposed via the medial capsule, and the anterior cruciate ligament (ACL) is completely transected (a). After joint instability confirmation, a bone tunnel is created in the anterior portion of the proximal tibia (b). Subsequently, a nylon thread is passed through the tunnel (c) and secured to the posterior aspect of the distal femur (d). To mitigate anterior translation of the tibia on the femur in the CAM group, the nylon thread is placed in the same orientation as the native ACL, providing a posteriorly directed traction force on the tibia that resists anterior motion over the condyles of the femur. In the SHAM model, the 3-0 nylon is loosely tied; therefore, the two models represent different joint instability. F: femur. T: tibia.

(Murata *et al*., 2019)

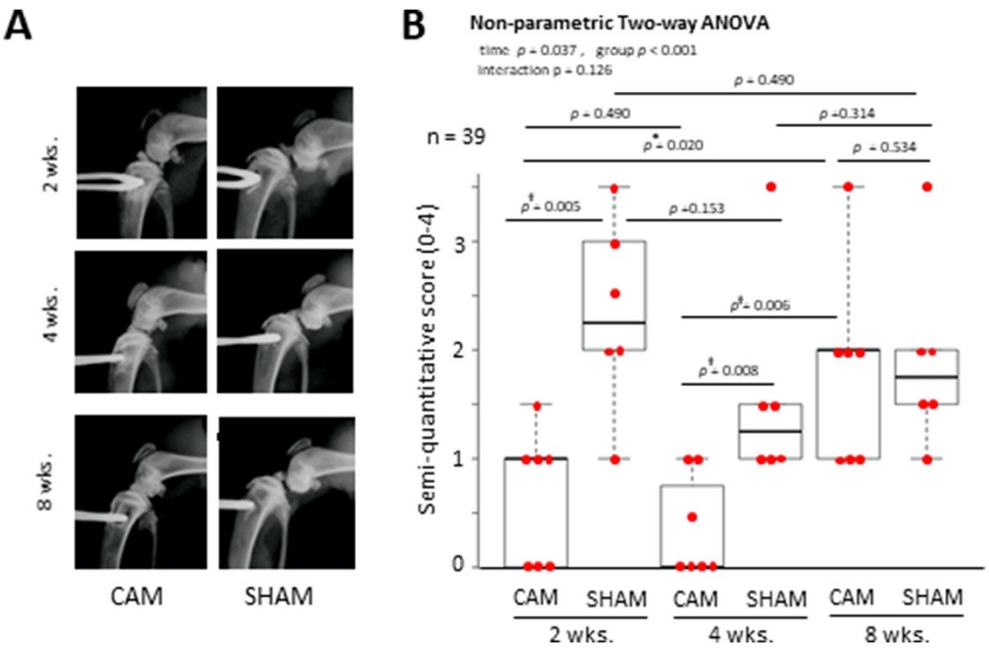

Fig. 13. Joint instability evaluation after surgery. (A) Soft radiographic images for joint instability (sagittal view) evaluated at 2, 4, and 8 weeks after surgery. Anterior translation of the tibia is increased in the SHAM group than in the CAM group. (B) There was a significant main effect for time and group (time: P = 0.037, group: P < 0.001; non-parametric two-way analysis of variance (ANOVA)). At 2 weeks and 4 weeks, the CAM group has significantly inhibited anterior tibial instability compared to the SHAM group (2 weeks, P = 0.005; 4 weeks, P = 0.008; post-hoc Manne-Whitney U test with Bonferroni-Holm correction); however no significant difference was observed between the SHAM and CAM groups at 8 weeks after surgery (P = 0.534; post-hoc Manne -Whitney U test with Bonferroni-Holm correction). The kappa coefficient reliability of the two evaluators of joint instability (Y.O. and T.K.) was 0.695. Boxplots show boxes extending from the 25th and 75th percentiles containing the median, with error bars down to the minimum and up to the maximum value. * <0.05, † <0.01.

(Murata *et al*., 2019)

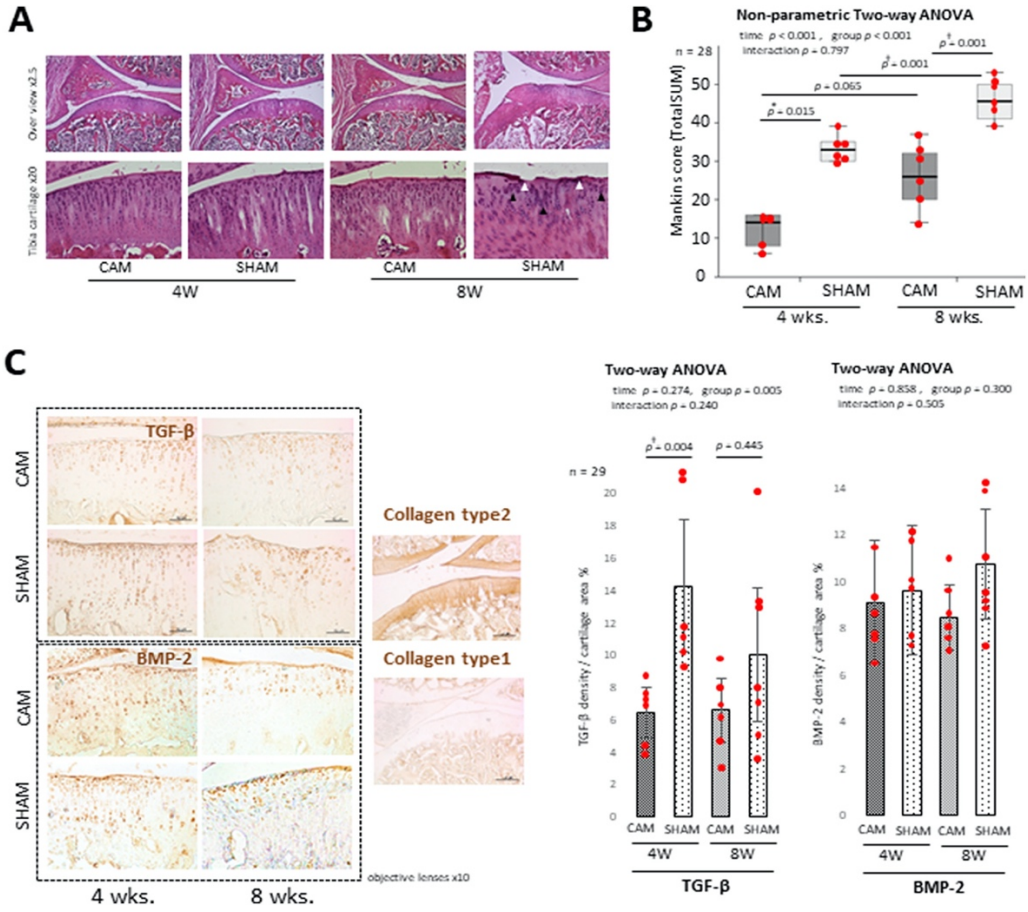

Fig. 14. Controlled abnormal joint movement delayed cartilage degeneration. (A) Histological sections of the cartilage stained with Mayer's hematoxylin and eosin. White arrowheads indicate cartilage pannus and fabrication of the cartilage surface. Black arrowheads indicate cartilage cell proliferation and/or cluster cells. (B) Mankin scores for histological osteoarthritic findings. The CAM group (controlled joint instability model) shows significantly lower score than the SHAM group (continued joint instability model) for the tibia (4 weeks, P = 0.015; 8 weeks, P = 0.001; post-hoc Manne-Whitney U test with Bonferroni-Holm correction). Boxplots show boxes extending from the 25th and 75th percentiles containing the median, with error bars down to the minimum and up to the maximum value. (C) The CAM section shows decreased TGF-β, bone morphogenetic protein (BMP)-2, and collagen type 2 and type 1 for positive control in the articular cartilage compared to that in the SHAM section at 8 weeks after surgery. In TGF-β, the semi-quantitative score for the tibia is significantly higher in the SHAM group than in the CAM group at 4 weeks (4 weeks, P = 0.004; post-hoc Games-Howell test); however no significant difference was observed between the SHAM and CAM groups at 8 weeks after surgery (P = 0.445; post-hoc Games-Howell test). Data are presented as means and 95% CIs. FA, femur anterior; FP, femur posterior; TA, tibia anterior; TP, tibia posterior; * <0.05, † <0.01.

(Murata *et al*., 2019)

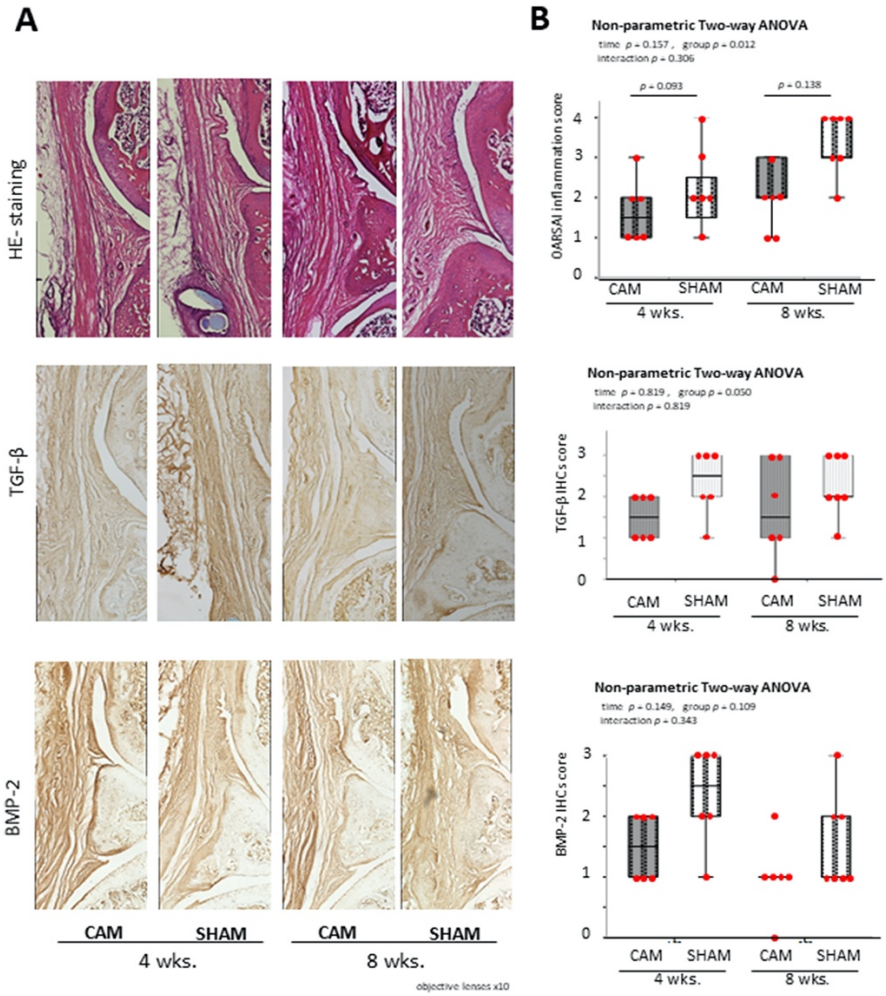

Fig. 15. Controlled abnormal joint movement shows inhibited synovial membrane inflammation and synovial thickening, TGF-β and BMP-2 IHC staining. (A) Histological sections of the synovial membrane stained using Mayer's hematoxylin and eosin. (B) The histological synovial inflammation scores and IHC staining scores were indicated. There was a significant main effect for group (P = 0.012; non-parametric two-way ANOVA); however no significant difference was observed between the SHAM and CAM groups at 4 weeks and 8 weeks after surgery (4 weeks, P = 0.093; 8weeks, P = 0.138; post-hoc Mann-Whitney U test with Bonferroni-Holm correction). TGF-β scores were not significantly higher in the CAM model than in the SHAM model (time, P = 0.819; group, P = 0.050; interaction, P = 0.819; non-parametric two-way ANOVA). BMP-2 expression was not significant difference between the two groups at 4 weeks and 8 weeks (time, P = 0.149; group, P = 0.109; interaction, P = 0.343; non-parametric two-way ANOVA). Boxplots show boxes extending from the 25th and 75th percentiles containing the median, with error bars down to the minimum and up to the maximum value. HE, hematoxylin and eosin; MM, medial meniscus; TGF-β, transforming growth factor-beta.

(Murata *et al*., 2019)

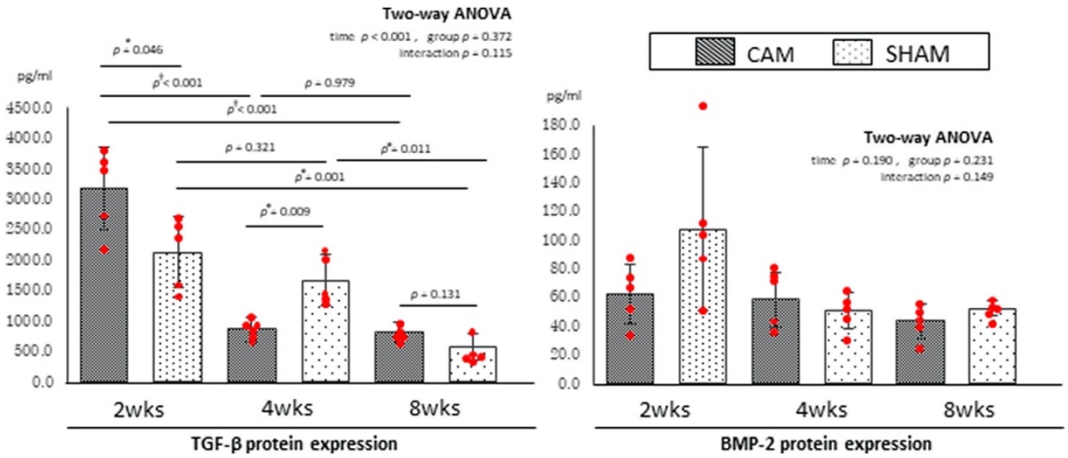

Fig. 16. ELISA results for TGF-β and BMP-2 expression levels in the synovial membrane. At 2 weeks after surgery, TGF-β levels are lower in the SHAM group than in the CAM group (n = 5 in each group; 2 weeks, P = 0.046); however, at 4 weeks after surgery, TGF-β levels are lower in the CAM group than in the SHAM group (n = 5 in each group; 4 weeks, P = 0.009). At 8 weeks after surgery no difference was found between the SHAM and CAM groups (n = 5 in each group; 8 weeks, P = 0.131). For BMP-2 levels, the groups show no significant difference at any time point (time, P = 0.190; group, P = 0.231, interaction, P = 0.149; two-way ANOVA). Data are presented as means and 95% CIs. BMP-2, BMP; CI, confidence interval; TGF-β, transforming growth factor-beta.

(Murata *et al*., 2019)

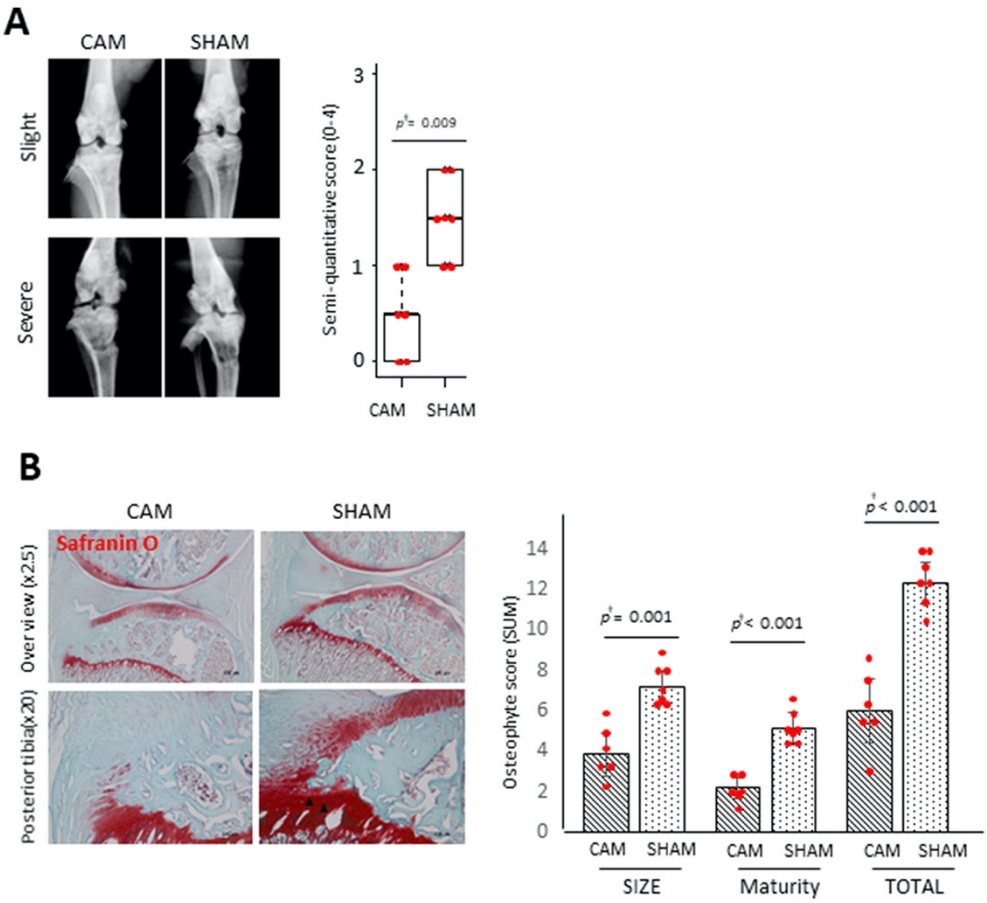

Fig. 17. Controlled abnormal joint movement inhibits osteophyte formation. (A) Soft radiographic images of osteophyte formation (frontal view) in the CAM and SHAM groups at 8 weeks after surgery. The semi-quantitative scores show significant increase in the SHAM group than in the CAM group (8 weeks, P = 0.009; Mann-Whitney U test). Boxplots show boxes extending from the 25th and 75th percentiles containing the median, with error bars down to the minimum and up to the maximum value. (B) Histological sections of the tibia posterior stained using Safranin O/fast green stains. Black arrowheads indicate chondroid metaplasia and osteophyte formation in the posterior tibia. Histological osteophyte formation scores. The CAM group shows significantly inhibited osteophyte size score and total score compared to those in the SHAM group (size score, P = 0.002; mature score, P < 0.001; total score, P < 0.001; Welch's *t* test). Data are presented as means and 95% CIs.

(Murata *et al*., 2019)

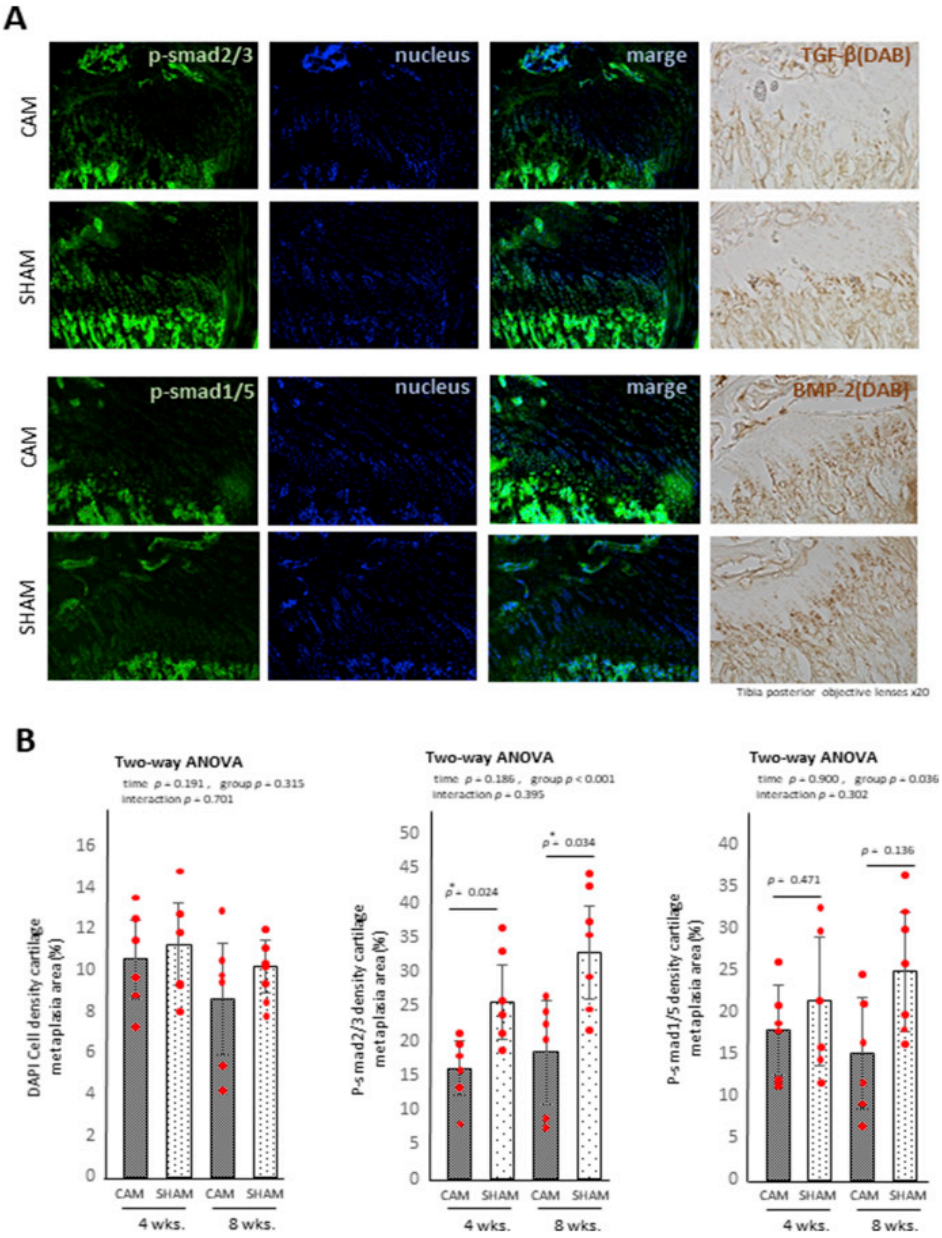

Fig. 18. Controlled abnormal joint movement inhibits p-Smad2/3 expression in cartilage metaplasia. (A) Immunofluorescence sections for anti-p-Smad2/3 and TGF-β, anti-p-Smad1/5/8 and BMP-2. The square area indicates the overexpression of p-Smad2/3 in cartilage metaplasia. TGF-β is also expressed in the same area. (B) Immunofluorescent density scores for p-Smad2/3, p-Smad1/5, and the nucleus. The CAM group has a significantly inhibited cartilage metaplasia score compared to that in the SHAM group at 4 and 8 weeks after surgery (4 weeks, P = 0.024; 8 weeks, P = 0.034; post-hoc Tukey test). p-Smad1/5 was markedly upregulated in the SHAM group than in the CAM group (4 weeks, P = 0.471; 8 weeks, P = 0.135; post-hoc Tukey test) and 8 weeks after surgery. Data are presented as means and 95% CIs. CI, confidence interval; TGF-β, transforming growth factor-beta.

(Murata *et al*., 2019)

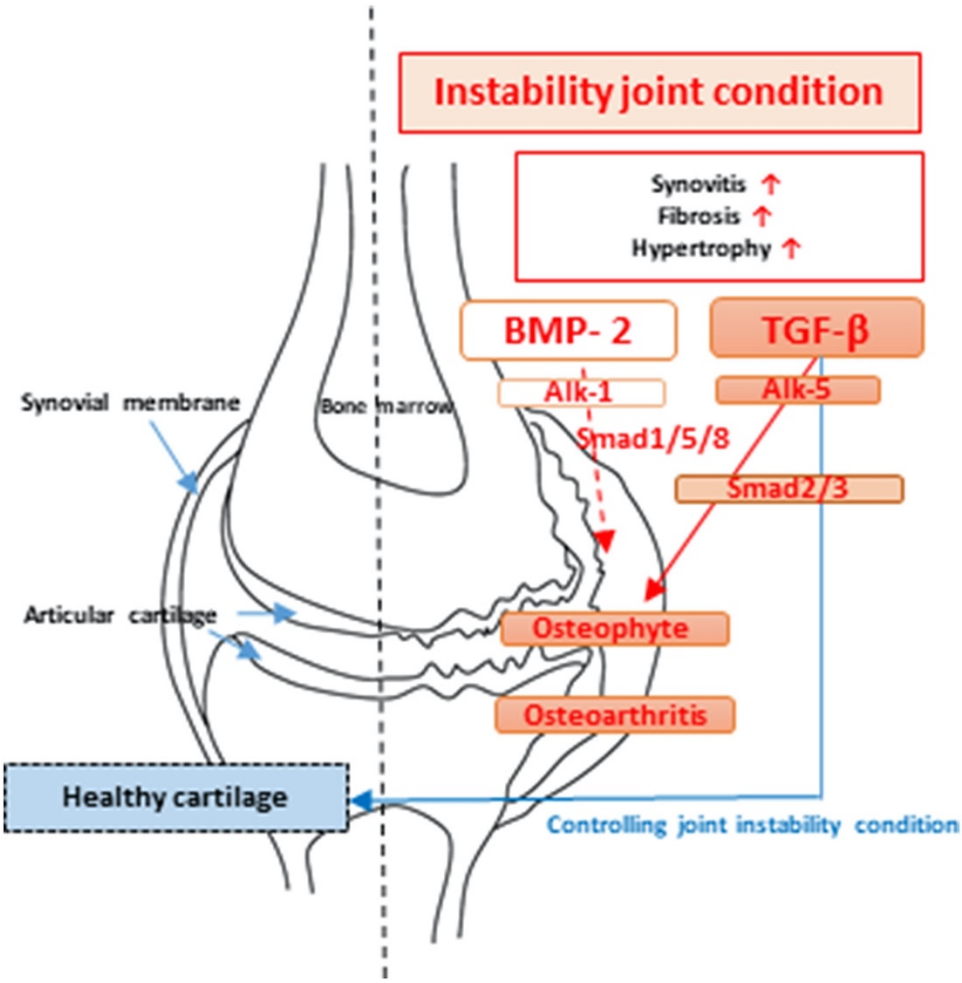

Fig. 19. Transforming growth factor-beta family and joint instability strategy for osteoarthritis cartilage and osteophyte formation.

(Murata *et al*., 2019)

Table 1
ICRS cartilage repair scores.

Standards	Points	Scores
Degree of defect repair	In level with surrounding cartilage	4
	75% repair of defect depth	3
	50% repair of defect depth	2
	25% repair of defect depth	1
	no repair of defect depth	0
Integration to border zone	Complete integration with surrounding cartilage	4
	Demarcating border < 1 mm	3
	75% repair tissue integrated, 25% with an evident border > 1 mm	2
	50% repair tissue integrated, 25% with an evident border > 1 mm	1
	From no contact to 25% repair tissue integrated with surrounding cartilage	0
Macroscopic appearance	Intact smooth surface	4
	Fibrillated surface	3
	Small, scattered fissures or cracks	2
	Several, small or few but large fissures	1
	Total degeneration of defect area	0

(Ying *et al*., 2018)

Table 2
Primer name and sequences for PCR analysis.

Primer name	Sequences
GAPDH forward	5′-GAACATCATCCCTGCATCCA-3′
GAPDH reverse	5′-CCAGTGAGCTTCCCGTTCA-3′
Col2a1 forward	5′-TCCTAAGGGTGCCAATGGTGA-3′
Col2a1 reverse	5′-AGGA CCAACTTTGCCTTGAGGAC-3′

(Ying *et al*., 2018)

Table3

Template and sequence of the primers used in this study.

Gene	Forward sequence (5′➔ 3′)	Reverse sequence(5′➔ 3′)
GAPDH	ATCTTCTTTTGCGTCGCCAG	TTCCCCATGGTGTCTGAGC
IL-6	AGCCCACCGGGAACGA	GGACCGAAGGCGCTTGT
IL-6R	GTACCACTGCCCACATTCCT	CCACGTCTTCTTGAACCTCAGA
RPS27a	GTTAAGCTGGCTGTCCTGAAA	CATCAGAAGGGCACTCTCG
SOCS3	TCGGACCAGCGCCACTT	CACTGGATGCGCAGGTTCT
SAA1	GTGATCAGCGATGCCAGAGA	TCGGAAGTGATTGGGGTCTT
BCL3	GGAGGCCCGCAATTATGA	CTTAATGTCCACTGCGTCGAT
MMP1	ACTGCCAAATGGGCTTGAAG	TTCCCTTTGAAAAACCGGACTT

(Wiegertjes *et al*., 2019)